

Supporting Information

Polymer of Intrinsic Microporosity based Macroporous Membrane with High Thermal Stability as Li-ion Battery Separator

Yangyang Tian^a, Chong Lin^c, Zhenggong Wang^{*b}, and Jian Jin^{*b,c}

^aSchool of Nano Technology and Nano Bionics, University of Science and Technology of China, Hefei 230026, China.

^bCollege of Chemistry, Chemical Engineering and Materials Science, Soochow University, Suzhou 215123, China.

^c*i*-Lab, Suzhou Institute of Nano-Tech and Nano-Bionics, Chinese Academy of Sciences, Suzhou 215123, China.

Supplemental Figures

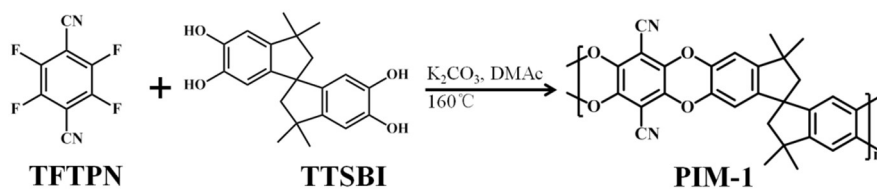


Figure S1. Synthesis route of PIM-1.

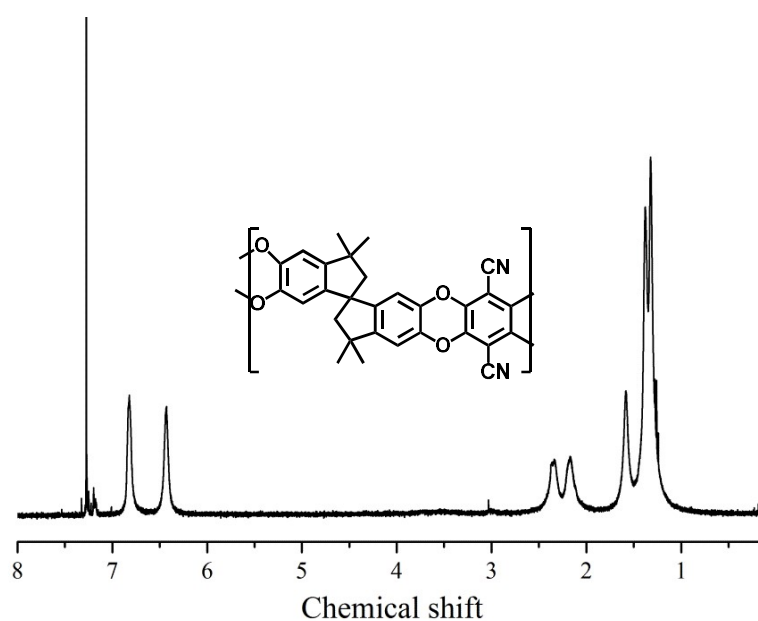


Figure S2. 1H NMR analysis of PIM-1 chemical structure.

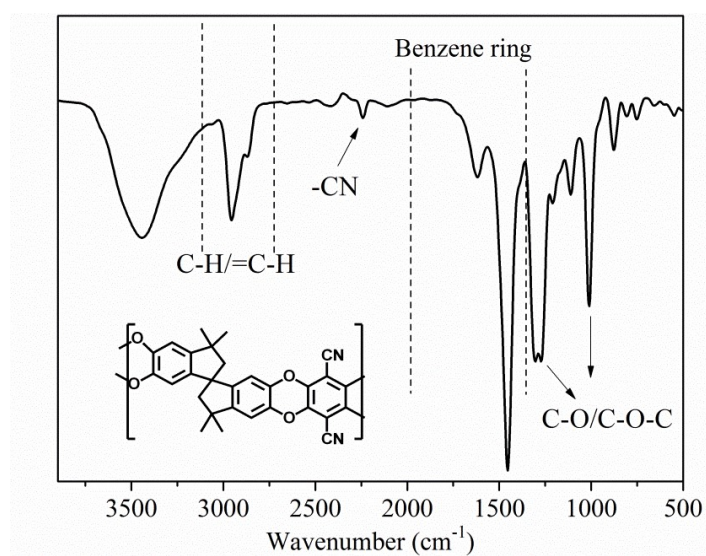


Figure S3. FT-IR spectrum of PIM-1.

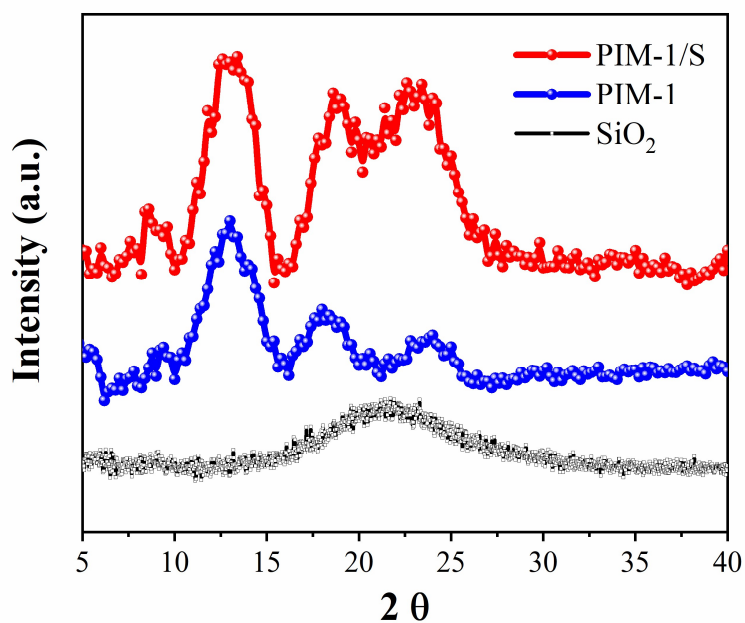


Figure S4. XRD pattern of PIM-1, PIM/S membrane and SiO₂ powder.

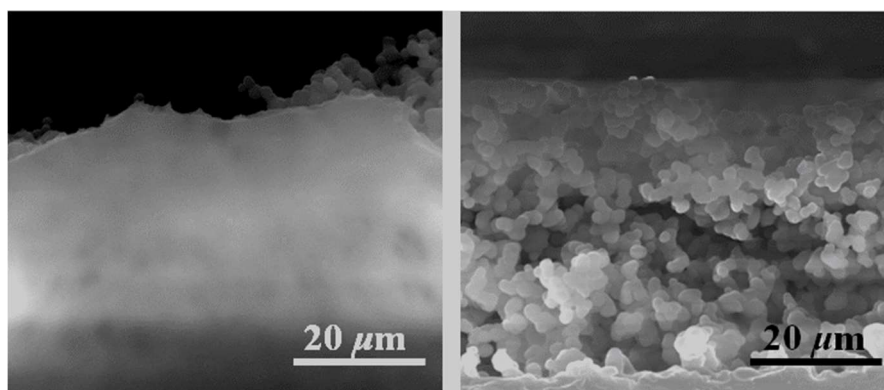


Figure S5. Surface (left) and cross-sectional (right) SEM images of PIM-1 membrane prepared by dry phase transition process without the addition of SiO₂ nanoparticles.

As shown in the above figures, the pure PIM-1 membrane without addition of SiO₂ nanoparticle demonstrates dense surface morphology. The phase transition phenomenon only occurs inside the membrane. Ultra-small size and -OH functionalized SiO₂ nanoparticle could furthermore slow down the non-solvent n-butyl alcohol evaporation. After the fast evaporation of CHCl₃, the adsorbed n-butyl

alcohol still exists inside the membrane. With temperature increase, the adsorbed n-butyl alcohol starts to evaporate and porous surface layer is successfully formed.

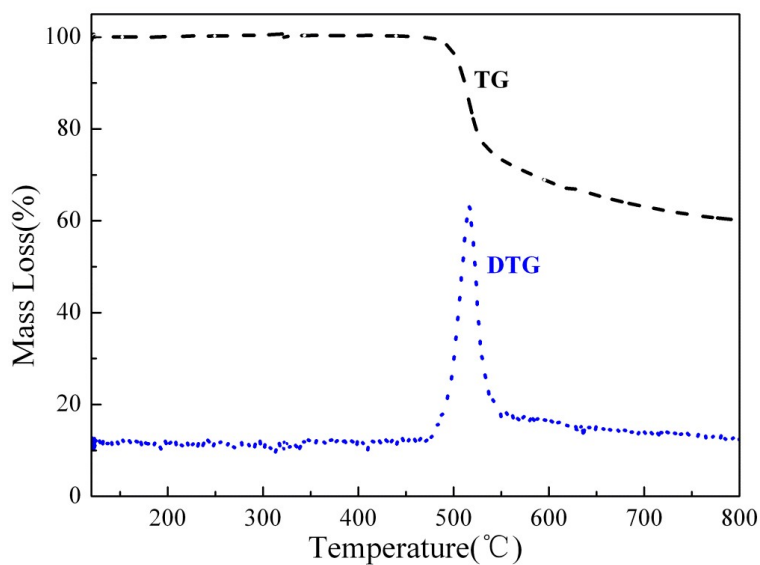


Figure S6. TGA and DTG curves of PIM-1.

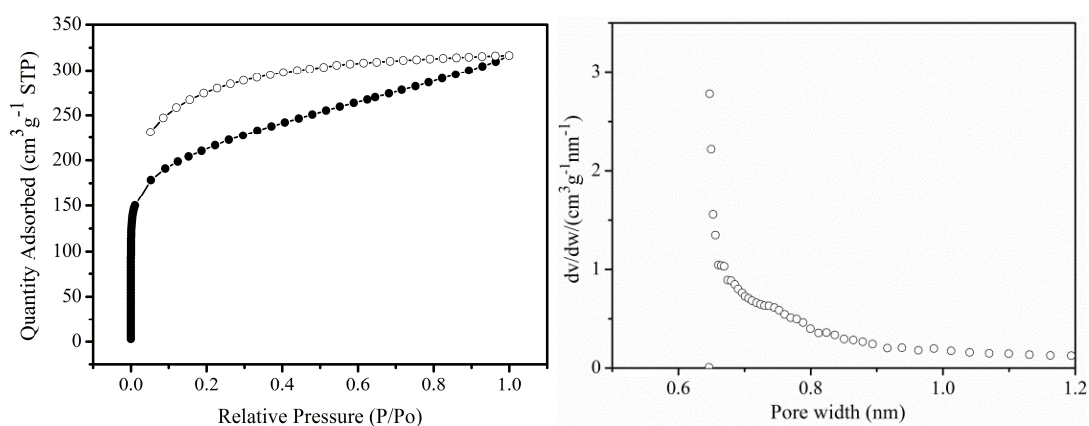


Figure S7. (a) N₂ adsorption (filled symbols) and desorption (open symbols) isotherms at 77 K for PIM-1; (b) pore width distribution obtained by analysis of N₂ adsorption by the Horvath-Kawazoe method.

The BET surface area of PIM-1 is 770 m²/g. Micropore around 0.7 nm is observed in the figure of pore width distribution.

Table S1. Physical properties of PP and PIM-1/S separators with different SiO₂ weight contents.

Sample	Porosity [%]	Electrolyte uptake [%]	Li-ion conductivity of cell [10^{-4} S cm ⁻¹ , 25°C]
PIM-1/S-0%	~39	~90	0.2
PIM-1/S-5%	~55	~150	3.2
PIM-1/S-10%	~67	~190	6.0
PIM-1/S-15%	~75	~240	8.2
PIM-1/S-20%	~81	~260	9.0
PP	~37	~110	5.1

The porosity was measured by immersing separators into isobutyl alcohol. After saturated adsorption, the solvent on the surface was wiped and then the weight of wet separator was recorded. The porosity was calculated following the equation (1):

$$\text{Porosity}(\%) = 100 \times \frac{\rho_m \times (M_s - M_d)}{\rho_m \times (M_s - M_d) + \rho_i \times M_d} \quad (1)$$

where ρ_m and ρ_i represent the density of the separator matrix and isobutyl alcohol. M_s and M_d represent the weight of the saturated and dry separator.

As shown in the table, the Li-ion conductivity and the electrolyte uptake capacity increase greatly with the increase of SiO₂ content. However, high SiO₂ content in the separator will sacrifice the mechanical strength of membrane. In our work, 15% SiO₂ content was chosen under the consideration of both the Li-ion conductivity and the electrolyte uptake and membrane strength.

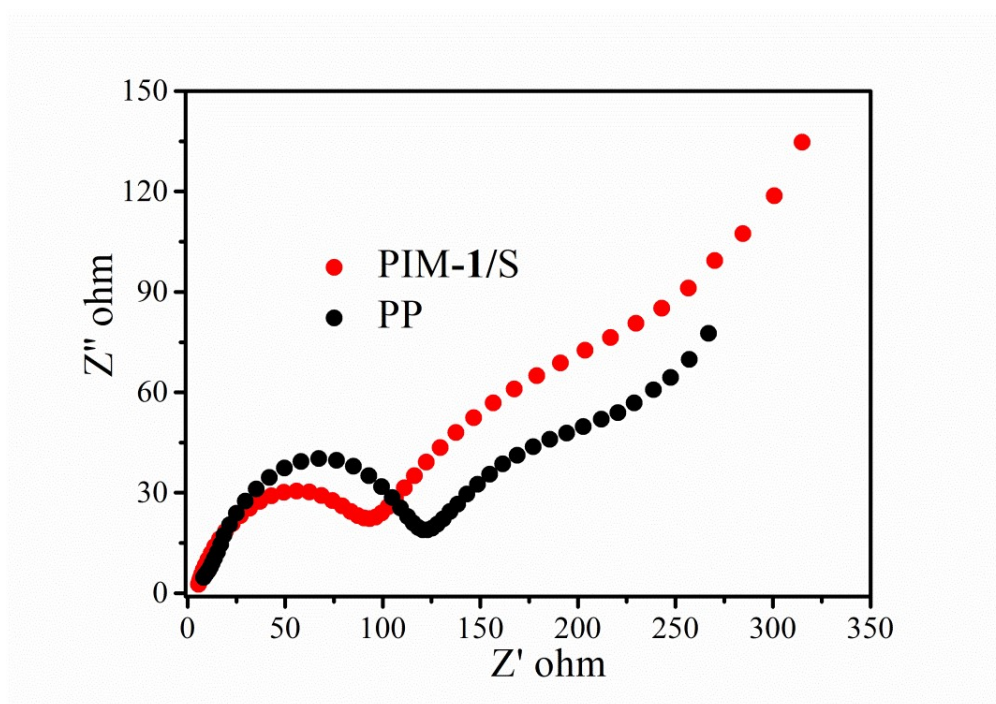


Figure S8. Nyquist plots of PIM-1/S and PP cells.